This article was downloaded by:
On: *14 January 2011*
Access details: *Access Details: Free Access*
Publisher *Taylor & Francis*
Informa Ltd Registered in England and Wales Registered Number: 1072954 Registered office: Mortimer House, 37-41 Mortimer Street, London W1T 3JH, UK

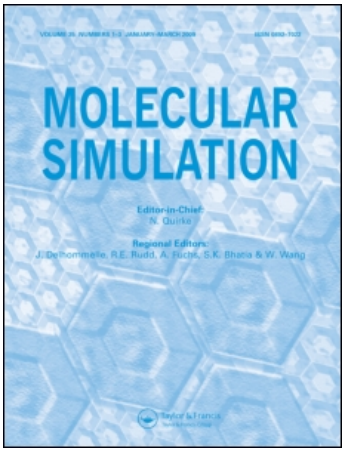

Molecular Simulation
Publication details, including instructions for authors and subscription information:
http://www.informaworld.com/smpp/title~content=t713644482

Density functional theory, restricted Hartree-Fock simulations and vibrational spectroscopic studies of nicorandil

R. Meenakshi[a]; Lakshmi Jaganathan[a]; S. Gunasekaran[b]; S. Srinivasan[c]
[a] Department of Physics, C.T.T.E. College for Women, Chennai, India [b] PG and Research Department of Physics, Pachaiyappa's College, Chennai, India [c] Department of Physics, L.N. Government College, Ponneri, India

Online publication date: 11 May 2010

To cite this Article Meenakshi, R. , Jaganathan, Lakshmi , Gunasekaran, S. and Srinivasan, S.(2010) 'Density functional theory, restricted Hartree-Fock simulations and vibrational spectroscopic studies of nicorandil', Molecular Simulation, 36: 6, 425 — 433
To link to this Article: DOI: 10.1080/08927020903583822
URL: http://dx.doi.org/10.1080/08927020903583822

PLEASE SCROLL DOWN FOR ARTICLE

Full terms and conditions of use: http://www.informaworld.com/terms-and-conditions-of-access.pdf

This article may be used for research, teaching and private study purposes. Any substantial or systematic reproduction, re-distribution, re-selling, loan or sub-licensing, systematic supply or distribution in any form to anyone is expressly forbidden.

The publisher does not give any warranty express or implied or make any representation that the contents will be complete or accurate or up to date. The accuracy of any instructions, formulae and drug doses should be independently verified with primary sources. The publisher shall not be liable for any loss, actions, claims, proceedings, demand or costs or damages whatsoever or howsoever caused arising directly or indirectly in connection with or arising out of the use of this material.

Molecular Simulation
Vol. 36, No. 6, May 2010, 425–433

Taylor & Francis
Taylor & Francis Group

Density functional theory, restricted Hartree–Fock simulations and vibrational spectroscopic studies of nicorandil

R. Meenakshi[a], Lakshmi Jaganathan[a], S. Gunasekaran[b] and S. Srinivasan[c]*

[a]*Department of Physics, C.T.T.E. College for Women, Chennai, India;* [b]*PG and Research Department of Physics, Pachaiyappa's College, Chennai 600 030, India;* [c]*Department of Physics, L.N. Government College, Ponneri 601 204, India*

(*Received 7 August 2009; final version received 28 December 2009*)

Fourier transform infrared and Raman spectra of nicorandil have been recorded. The structure, conformational stability, geometry optimisation and vibrational frequencies have been investigated. Complete vibrational assignments were made for the stable conformer of the molecule using restricted Hartree–Fock (RHF) and density functional theory (DFT) calculations (B3LYP) with the 6-31G(d,p) basis set. Comparison of the observed fundamental vibrational frequencies of the molecule and calculated results by RHF and DFT methods indicates that B3LYP is superior for molecular vibrational problems. The thermodynamic functions of the title molecule were also performed using the RHF and DFT methods. Natural bond order analysis of the title molecule was also carried out. Comparison of the simulated spectra with the experimental spectra provides important information about the ability of the computational method to describe the vibration modes.

Keywords: nicorandil; vibrational spectra; restricted Hartree–Fock; density functional theory

Downloaded At: 17:09 14 January 2011

1. Introduction

Nicorandil is a nicotinamide nitrate used as an antianginal agent. It is chemically known as *N*-[2-nitroxy ethyl]-3-pyridine carboxamide, which belongs to the class of compounds known as potassium channel activators. Nicorandil has venodilating properties (i.e. relaxing the smooth muscle of the blood vessels) owing to the presence of the nitrate group in its structure. The potassium channel activation may also exert direct cytoprotective effects by augmenting a normal physiological process, which protects heart against ischaemic events [1,2].

To our knowledge, no theoretical Hartree–Fock (HF) or density functional theory (DFT) calculations or detailed vibrational infrared (IR) and Raman analyses have been performed on the nicorandil molecule. A detailed quantum chemical investigation will aid in understanding the vibrational modes of nicorandil and clarifying the experimental data available for this molecule. DFT calculations are known to provide excellent vibrational wavenumbers scaled to compensate for the approximate treatment of electron correlation, for basis set deficiencies and anharmonicity effects [3–8]. DFT is the best method rather than the *ab initio* method for the computation of molecular structure, vibrational wavenumbers and energies of molecules [9]. In this work, by using the HF and B3LYP methods, we calculated the vibrational wavenumbers of nicorandil and molecular geometric parameters. These calculations are valuable for providing insight into the vibrational spectrum and molecular parameters.

2. Experimental

The spectroscopic pure sample of nicorandil was procured from reputed pharmaceutical firms in Chennai, India and used as such without any further purification. The Fourier transform infrared (FTIR) spectrum of nicorandil was recorded on an ABB Bomem Series spectrometer over the region $4000–400\,cm^{-1}$ by adopting the KBr pellet technique at Dr Ceeal Analytical Lab, Chennai, India. The FT-Raman spectrum was recorded on a Nexus 670 spectrometer at Central Electro Chemical Research Institute Laboratory, Karaikudi, India. The laser frequency of $15{,}798\,cm^{-1}$ was used as the excitation source. The spectrometer is fitted with an XT-KBr beam splitter and a DTGS detector. A baseline correction was made for the spectrum recorded.

3. Computation

All the theoretical computations were performed at restricted HF (RHF) and B3LYP levels on a Pentium IV/1.6 GHz personal computer using the Gaussian 03W program package [10]. The geometries were first optimised at the RHF level of theory employing the 6-31G(d,p) basis set. DFT employed the B3LYP keyword, which invokes Becke's three-parameter hybrid method [9] using the correlation function of Lee et al. [11]. Polarisation functions were added for a better description of polar bonds of amino and nitro groups. The optimised geometry was used in the vibrational frequency calculations at the

*Corresponding author. Email: dr_s_srinivasan@yahoo.com

ISSN 0892-7022 print/ISSN 1029-0435 online
© 2010 Taylor & Francis
DOI: 10.1080/08927020903583822
http://www.informaworld.com

RHF and DFT levels to characterise all stationary points as minima. Finally, calculated normal-mode vibrational frequencies provide thermodynamic properties by way of statistical mechanics. The vibrational frequency assignments were made with a high degree of accuracy with the help of Chemcraft software program (Chem3D Ultra 8.0, Cambridgesoft.com, Cambridge, MA, USA).

4. Results and discussion

4.1 Molecular geometry

The optimised molecular structure for nicorandil in the ground state (*in vacuo*) was computed by RHF and B3LYP calculations with the 6-31G(d,p) basis set. The values of the total energy for nicorandil, obtained from the RHF and B3LYP calculations by employing the 6-31G(d,p) basis set, are found to be -770.84 a.u. (2.032×10^6 kJ/mol) and -775.30 a.u. (2.043×10^6 kJ/mol), respectively. The calculated geometrical parameters (bond lengths and bond angles) were compared with experimentally obtained X-ray diffraction (XRD) data values [12]. As the experimental values for nicorandil are known, the theoretically calculated values may give an idea about the geometry of these molecules and also an idea of how the geometry of the molecule changes from the *ab initio* method of calculation and the DFT method of calculation. The optimised structural parameters of nicorandil from the RHF/6-31G(d,p) and B3LYP/6-31G(d,p) calculations and the XRD values are listed in Table 1, in accordance with the atom numbering scheme given in Figure 1. The slight deviation in XRD data from the computed geometry is probably due to the fact that the intermolecular interactions in the crystalline state are dominant. The B3LYP method leads to geometry parameters, which are close to experimental data [12]. A statistical treatment of these data shows that, for the bond lengths, B3LYP/6-31G(d,p) is better than the RHF/6-31G(d,p) geometry. The correlation coefficients for bond lengths computed from the DFT and RHF methods with the experimental values were found to be 0.9809 and 0.9709, respectively. Similarly, the correlation coefficients for bond angles computed from the DFT and RHF methods with the experimental values were found to be 0.9335 and 0.8851, respectively. It can be noted from the correlation coefficient values that the theoretical predictions are not in good agreement with the experimental value for bond angles.

4.2 Bond order analysis

The bond order of nicorandil is presented in Table 2. Bond order is related to bond strength. The bonds with the higher bond order values have short bond length and vice versa.

Downloaded At: 17:09 14 January 2011

Table 1. Comparison between the RHF and DFT calculated and experimental values of geometrical parameters of nicorandil.

Bond length (Å)				Bond angle (°)			
	DFT	RHF	Reference [12]		DFT	RHF	Reference [12]
C_1—C_2	1.399	1.387	1.381	C_4—N_6—C_5	117.3	118.0	116.7
C_1—C_3	1.392	1.382	1.385	C_3—C_5—N_6	123.7	123.6	124.0
C_1—H_{16}	1.087	1.076	–	C_1—C_3—C_5	118.4	118.2	118.6
C_2—C_4	1.403	1.392	1.394	C_3—C_1—C_2	118.9	118.9	118.8
C_2—C_7	1.499	1.496	1.493	C_1—C_2—C_4	117.8	117.8	117.9
C_3—C_5	1.396	1.384	1.383	C_1—C_2—C_7	124.5	124.3	124.8
C_3—H_{17}	1.085	1.074	–	C_4—C_2—C_7	117.8	118.0	117.4
C_4—N_6	1.335	1.318	1.335	C_2—C_4—N_6	123.9	123.6	124.0
C_4—H_{18}	1.087	1.074	–	C_2—C_7—O_9	122.0	121.7	120.4
C_5—N_6	1.340	1.322	1.328	C_2—C_7—N_8	116.4	116.7	117.3
C_5—H_{19}	1.088	1.076	–	O_9—C_7—N_8	121.6	121.7	122.3
C_7—N_8	1.374	1.361	1.337	C_7—N_8—C_{10}	120.2	120.4	121.5
C_7—O_9	1.227	1.201	1.236	N_8—C_{10}—C_{11}	110.7	110.4	112.5
N_8—C_{10}	1.456	1.449	1.450	C_{10}—C_{11}—O_{12}	104.8	104.3	111.7
N_8—H_{20}	1.008	0.992	–	C_{11}—O_{12}—N_{13}	113.8	116.4	114.7
C_{10}—C_{11}	1.530	1.520	1.510	O_{12}—N_{13}—O_{14}	112.7	113.9	113.7
C_{10}—H_{21}	1.094	1.082	–	O_{12}—N_{13}—O_{15}	117.4	117.9	118.4
C_{10}—H_{22}	1.093	1.082	–	O_{14}—N_{13}—O_{15}	129.9	128.1	127.9
C_{11}—O_{12}	1.445	1.436	1.459	CC	0.9335	0.8851	
C_{11}—H_{23}	1.094	1.080	–				
C_{11}—H_{24}	1.092	1.078	–				
O_{12}—N_{13}	1.416	1.329	1.382				
N_{13}—O_{14}	1.206	1.178	1.198				
N_{13}—O_{15}	1.214	1.186	1.204				
CC	0.9809	0.9709					

Note: CC, correlation coefficient.

Figure 1. Atom numbering scheme of nicorandil.

The bond order analysis may predict that the weakest bonds may be cleaved preferentially and they may possess a relatively low π-bond character. The bond order values of C—C and C—N bonds in pyridine rings show that they have delocalised double bond characteristics. The bond order value of C_7—N_8 shows single bond nature. The N_{13}—O_{14} and N_{13}—O_{15} bond order values are in the range 1.5, which depict the double bond character, while the N_{13}—O_{12} bond order value is approximately unity, which shows the single bond character. The optimised geometrical values are in support of the bond order analysis.

4.3 *Natural population analysis*

The calculation of effective atomic charges plays an important role in the application of quantum mechanical calculations to molecular systems. Our interest here is in the comparison of different methods (RHF and DFT) to describe the electron distribution in nicorandil as broadly as possible, and to assess the sensitivity of the calculated charges to changes in the choice of the quantum chemical method. The calculated natural atomic charge values from the natural population analysis (NPA) and Mulliken population analysis (MPA) procedures using the RHF and DFT methods are listed in Table 3. The NPA from the natural bonding orbital (NBO) method is better than the MPA scheme. Table 3 compares the atomic charge site of nicorandil from both MPA and NPA methods. The NPA of nicorandil shows that the presence of three oxygen atoms in the nitrate moiety [$O_{12} = -0.448$ (RHF) and -0.402 (DFT); $O_{14} = -0.426$ (RHF) and -0.333 (DFT); $O_{15} = -0.469$ (RHF) and -0.367 (DFT)] imposes large positive charges on the nitrogen atom [$N_{13} = 0.935$ (RHF) and 0.748 (DFT)]. However, the nitrogen atoms N_6 and N_8 possess large negative charges, resulting in the positive charges on the carbon atoms C_4, C_5 and C_7. Moreover, there is no difference in charge distribution observed on all hydrogen atoms except the H_{20} hydrogen atom ($H_{20} = 0.426$ in RHF and 0.425 in DFT). The large positive charge on H_{20} is due to the large negative charge accumulated on the N_8 atom.

Table 2. Bond orders of nicorandil.

Bond order	B3LYP/6-31G(d,p)	RHF/6-31G(d,p)
C_1—C_2	1.3939	1.4021
C_1—C_3	1.4405	1.4385
C_1—H_{16}	0.9115	0.9181
C_2—C_4	1.3670	1.3698
C_2—C_7	1.0007	0.9925
C_3—C_5	1.4256	1.4249
C_3—H_{17}	0.9080	0.9150
C_4—N_6	1.4442	1.4330
C_4—H_{18}	0.8963	0.9061
C_5—N_6	1.4163	1.4069
C_5—H_{19}	0.9083	0.9169
C_7—N_8	1.1580	1.1191
C_7—O_9	1.6558	1.6366
N_8—C_{10}	0.9664	0.9581
N_8—H_{20}	0.7887	0.7948
C_{10}—C_{11}	0.9931	0.9987
C_{10}—H_{21}	0.8925	0.9083
C_{10}—H_{22}	0.9116	0.9240
C_{11}—O_{12}	0.8683	0.8241
C_{11}—H_{23}	0.9127	0.9259
C_{11}—H_{24}	0.9005	0.9146
O_{12}—N_{13}	0.9052	0.9918
N_{13}—O_{14}	1.5751	1.5762
N_{13}—O_{15}	1.5409	1.5312

4.4 *Vibrational spectral assignment*

From the optimised geometry, it is observed that the nicorandil molecule belongs to the C_1 symmetry and hence all the 66 modes of vibrations are both IR and Raman active. In the present work, FTIR and FT-Raman spectra of nicorandil have been recorded (see Figures 2 and 3, respectively). Owing to the lack of sufficiently detailed experimental data for the nicorandil molecule, the vibrational spectra were obtained by the RHF and DFT calculations. Figures 4 and 5 show the theoretically simulated vibrational spectrum of nicorandil by the DFT and RHF methods, respectively. Because of the low IR and Raman intensity of some modes, it is difficult to observe them in the IR and Raman spectra. The RHF and DFT calculations have been carried out to estimate the fundamental vibrational frequencies. The calculated vibrational mode frequencies of nicorandil were compared with the observed frequencies. The assignments of the vibrational absorptions were made by using Chemcraft software program (Chem3D Ultra 8.0, Cambridgesoft.com). Calculations were made for a free molecule in vacuum, while experiments were performed for solid samples, so that there are disagreements between the calculated and observed vibrational wavenumbers. The scaling factors 0.960 and 0.899 for the DFT and RHF values, respectively, have to be necessarily used to find a good agreement with the experimental values [13]. The DFT values were found to be in good agreement with the

Downloaded At: 17:09 14 January 2011

Table 3. Natural atomic charges of nicorandil.

	MPA		NPA	
Atom with numbering	RHF/6-31G(d,p)	B3LYP/6-31G(d,p)	RHF/6-31G(d,p)	B3LYP/6-31G(d,p)
C_1	−0.074	−0.087	−0.149	−0.195
C_2	−0.208	0.020	−0.237	−0.181
C_3	−0.215	−0.102	−0.305	−0.275
C_4	0.174	0.095	0.131	0.066
C_5	0.144	0.104	0.094	0.030
N_6	−0.542	−0.433	−0.508	−0.442
C_7	0.797	0.560	0.844	0.68
N_8	−0.755	−0.554	−0.753	−0.667
O_9	−0.605	−0.513	−0.715	−0.613
C_{10}	−0.045	−0.076	−0.235	−0.292
C_{11}	0.110	0.071	−0.067	−0.142
O_{12}	−0.532	−0.401	−0.448	−0.402
N_{13}	0.981	0.756	0.935	0.748
O_{14}	−0.443	−0.354	−0.426	−0.333
O_{15}	−0.473	−0.366	−0.469	−0.367
H_{16}	0.169	0.097	0.235	0.239
H_{17}	0.168	0.102	0.244	0.250
H_{18}	0.200	0.137	0.244	0.249
H_{19}	0.164	0.110	0.224	0.231
H_{20}	0.314	0.266	0.426	0.425
H_{21}	0.180	0.157	0.245	0.261
H_{22}	0.149	0.122	0.231	0.247
H_{23}	0.151	0.125	0.218	0.230
H_{24}	0.188	0.161	0.241	0.253

Downloaded At: 17:09 14 January 2011

experimental values after scaling the vibrational frequencies in comparison to the RHF values. The calculated and experimental wavenumbers and intensities for all the fundamental modes of vibration for nicorandil with their corresponding vibrational assignments are given in Table 4.

4.5 N—H stretching modes

Secondary amides show only one N—H stretching band while primary amides display two N—H stretching modes due to symmetrical and asymmetrical stretching modes of vibrations. From the IR spectroscopy of secondary amides, free N—H stretching vibrations are observed in the range 3500–3400 cm^{-1} in dilute concentrations and, in solid samples, these bands are shifted to 3350–3200 cm^{-1} [14]. Azhagiri et al. [15] have assigned the N—H stretching vibration in the region 3500–3750 cm^{-1} for the gas-phase 2-nitroaniline by both DFT and RHF methods. With this analogy, a sharp, strong intense band at 3245 cm^{-1} in the FTIR spectrum and a weak intense band at 3251 cm^{-1} in the FT-Raman spectrum have been assigned to N—H stretching vibrations, which is calculated near 3513 cm^{-1} in the DFT method and 3520 cm^{-1} in the RHF method.

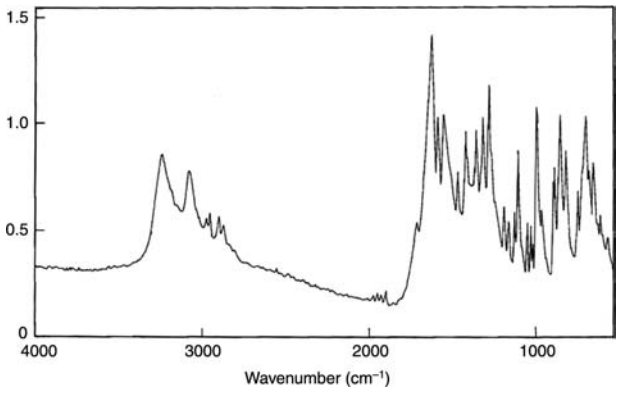

Figure 2. FTIR spectrum of nicorandil.

4.6 C—H stretching modes

Floare et al. [16] assigned the weak to medium intensity bands observed at 3000–3100 cm^{-1} in the IR spectrum and the medium to strong intensity bands in the above region in the Raman spectrum to C—H stretching vibrations in the pyridine ring. Also, the normal coordinate analysis of some pyridine reported by Venkatram Reddy and Ramana Rao [17] identified that the bands at 3080 and 3036 cm^{-1} are due to C—H stretching vibrations. With this view, the bands observed at 3077 and 3018 cm^{-1} in the FTIR spectrum and 3094, 3059, 3017 and 3000 cm^{-1} in the FT-Raman spectrum were assigned to C—H stretching vibrations in the pyridine ring CH modes. The DFT calculation correlates with the experimental assignment

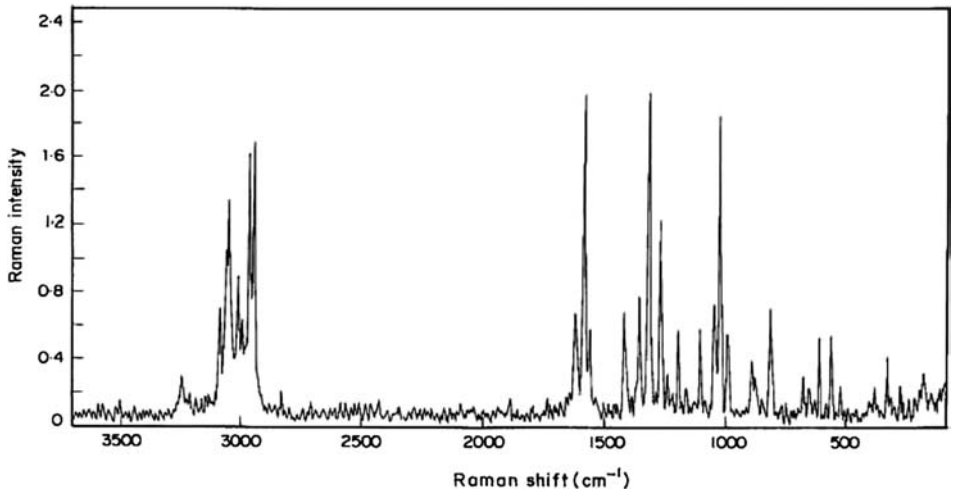

Figure 3. FT-Raman spectrum of nicorandil.

Downloaded At: 17:09 14 January 2011

better than the RHF method. The methyl C—H stretching vibrational modes are assigned to lower wavenumbers. The corresponding calculated values fall in the same region. The corresponding computed bands at 2952, 2961, 3005 and 3029 cm^{-1} in DFT values and 2913, 2940, 2961 and 3011 cm^{-1} in RHF values are due to CH stretching vibrations of methyl group present in the molecule. These C—H stretching vibrations are pure modes.

4.7 C═O and N═O, and C═C stretching vibrations

The C═O stretching is assigned at 1692 and 1750 cm^{-1} in the DFT and RHF methods, respectively, meanwhile in the FTIR and FT-Raman spectra, the assignment goes to 1717 and 1720 cm^{-1}, respectively. In the FTIR spectrum, the N═O stretching is assigned at 1629 cm^{-1}, whereas in the FTIR spectrum, it is assigned at 1630 cm^{-1}. The DFT calculations assigning these N═O stretching at 1689 cm^{-1} give a deviation of 3.6%, and the RHF calculations at 1716 cm^{-1} have a deviation of 5.3%. The above results are in agreement with the literature [18]. The bands observed at 1558 and 1591 cm^{-1} in the FTIR spectrum and at 1569 and 1592 cm^{-1} in the Raman spectrum are ascribed to the C═C stretching mode. These vibrations are predicted at 1557 and 1579 cm^{-1} by DFT calculations for nicorandil, which agree well with the experimental values. Our calculations predicted that the intense bands observed at 1373 cm^{-1} in the FTIR spectrum and 1363 cm^{-1} in the Raman spectrum have resulted from the interaction of C═C stretching and CCH bending vibration of the pyridine ring group.

4.8 C—N and C—C stretching vibrations

The intense bands observed in the FTIR and FT-Raman spectra at 1324 cm^{-1} are attributed to CC and CN stretching vibrations. A very strong band observed at 1277 cm^{-1} in the Raman spectra, and also observed as an intense band at 1289 cm^{-1} in the FTIR spectrum, resulted from the

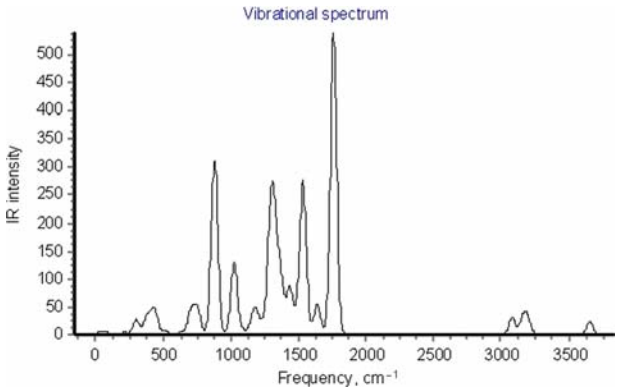

Figure 4. DFT-simulated IR spectrum of nicorandil.

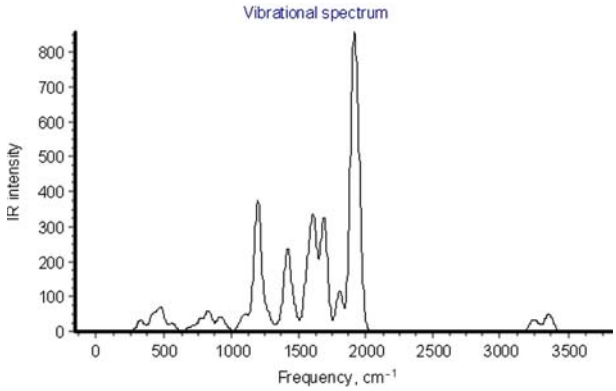

Figure 5. RHF-simulated IR spectrum of nicorandil.

Downloaded At: 17:09 14 January 2011

Table 4. Comparison of the calculated and experimental wavenumbers (cm^{-1}) and intensities (km/mol) of nicorandil.

	Observed wavenumbers		Calculated wavenumbers						
			B3LYP/6-31G(d,p)			RHF/6-31G(d,p)			
Modes	FTIR	FT-Raman	Unscaled frequency	Scaled frequency	Intensity	Unscaled frequency	Scaled frequency	Intensity	Vibrational band assignment
1			26	25	2.5	31	28	2.2	ONO bending/CCN bending
2			34	33	0.3	38	34	0.8	ONO bending
3			41	39	0.7	44	40	0.8	ONO bending
4			60	58	2.2	71	64	3.5	NOC bending
5			87	84	2.6	106	95	2.7	ONO bending/CCO bending
6		104 (vw)	134	129	1.3	146	131	1.1	CCN bending
7			149	143	1.3	162	146	2.4	ONO bending/CCO bending
8			165	158	1.3	173	156	0.8	CCO bending/NOC bending
9		197 (vw)	209	201	3.5	232	209	4.3	CCN bending
10			249	239	1.3	272	245	0.8	CCC bending
11		291 (vw)	299	287	27.6	329	296	33.2	CCC bending
12		345 (w)	366	351	10.2	409	368	20.9	C—NH bending
13			382	367	22.4	425	382	23.8	NO_2 rocking
14		397 (vw)	410	394	9.5	455	409	9.8	CH wagging
15			434	417	37.3	475	427	45	NH wagging
16			454	436	5	496	446	20.7	CNC bending
17			515	494	7.6	564	507	22.8	CC stretching/COC bending
18	576 (m)	577 (m)	626	601	2.5	679	610	3.2	CC stretching/CO stretching
19	620 (s)	621 (m)	634	609	1.9	708	636	11.7	CH wagging
20	665 (s)	663 (vw)	699	671	35.4	769	691	10.9	CCC bending
21	689 (s)	689 (w)	717	688	0.9	775	697	23.4	CC torsion
22			722	693	9.8	828	744	2.8	CC torsion
23	707 (s)		746	716	31.6	835	751	53.9	CH wagging
24	728 (m)		761	731	15.6	849	763	1.2	NO_2 wagging
25	755 (m)		785	754	0.2	913	821	31.8	CH wagging
26	825 (m)	822 (m)	835	802	5	925	832	5	HCCH bending
27			877	842	182.3	953	857	18	NO_2 scissoring
28			882	847	130.1	1075	966	25.1	CCC bending
29	899 (m)	899 (m)	962	924	0.7	1083	974	1.7	CCH bending
30			982	943	2.4	1103	992	7	CH wagging
31			1005	965	1.3	1114	1001	25.4	CCH bending
32			1019	978	58.1	1121	1008	5.6	COC bending/CCH bending
33	969 (w)		1029	988	74.5	1138	1023	0.2	CH wagging
34	1002 (s)	1001 (m)	1046	1004	1.1	1154	1037	2.6	CCC bending
35	1034 (m)	1033 (vs)	1075	1032	1.1	1182	1063	47.3	CH wagging
36	1058 (m)	1055 (m)	1090	1046	6.1	1198	1077	323.7	CH wagging/CN stretching
37			1146	1100	9.3	1200	1079	8.6	CH wagging
38	1112 (s)	1112 (m)	1159	1113	2.8	1249	1123	31.1	NH wagging/CH wagging
39	1135 (w)		1181	1134	43.7	1269	1141	24.4	CCC bending
40	1170 (w)	1169 (vw)	1231	1182	11.6	1285	1155	13.1	CH_2 twisting/HCC bending

Downloaded At: 17:09 14 January 2011

Table 4 – *continued*

Modes	Observed wavenumbers		Calculated wavenumbers						Vibrational band assignment
			B3LYP/6-31G(d,p)			RHF/6-31G(d,p)			
	FTIR	FT-Raman	Unscaled frequency	Scaled frequency	Intensity	Unscaled frequency	Scaled frequency	Intensity	
41	1197 (m)	1202 (m)	1246	1196	9.4	1338	1203	9.8	CH_2 twisting/HCC bending
42			1294	1242	185.8	1366	1228	14.9	HCC bending
43			1307	1255	0.5	1415	1272	217	HCC bending
44	1260 (m)	1248 (w)	1323	1270	131.8	1449	1303	35.1	CH_2 twisting/HCC bending
45	1289 (s)	1277 (vs)	1340	1286	16.3	1474	1325	37.1	CN stretching/HNC bending/HCC bending
46			1364	1309	2.9	1477	1328	2.3	CC and CN stretching
47	1324 (s)	1324 (vs)	1369	1314	95.4	1558	1401	115.3	CC and CN stretching
48	1373 (s)	1363 (m)	1432	1375	72.7	1579	1420	27.1	C═C stretching+CCH bending
49			1456	1398	20.6	1609	1446	290.2	C═C stretching+CCH bending
50	1426 (s)	1427 (m)	1490	1430	7.4	1623	1459	4.7	CH_2 scissoring
51			1513	1452	39.3	1644	1478	38.9	HCH bending
52			1530	1469	4.5	1657	1490	4.8	HCH bending
53	1473 (m)	1423 (m)	1537	1476	245.8	1690	1519	315.4	CN and CC stretching
54	1558 (s)	1569 (m)	1622	1557	15.8	1782	1602	22.5	C═C stretching
55	1591 (s)	1592 (vs)	1645	1579	43.8	1809	1626	102.6	C═C stretching
56	1629 (vs)	1630 (m)	1759	1689	373.5	1909	1716	748.8	N═O stretching
57	1717 (s)	1720 (w)	1763	1692	168.1	1947	1750	309.3	C═O stretching
58	2955 (m)	2954 (vs)	3075	2952	7.4	3240	2913	26.4	CH stretching
59	2974 (m)	2972 (vs)	3084	2961	23.5	3270	2940	12.3	CH stretching
60		3000 (vs)	3130	3005	2.1	3294	2961	7.6	CH stretching
61	3018 (m)	3017 (s)	3155	3029	12	3349	3011	10.6	CH stretching
62			3172	3045	15.3	3350	3012	7.2	CH stretching
63		3059 (s)	3184	3057	13.8	3358	3019	23.8	CH stretching
64			3200	3072	3	3384	3042	16.4	CH stretching
65	3077 (s)	3094 (s)	3212	3084	12.6	3389	3047	0.4	CH stretching
66			3659	3513	23.4	3915	3520	41.7	NH stretching

interaction between N—H bending and C—N stretching and CCH bending vibrations of CNH and CCH groups.

4.9 Bending vibrations

The deformation vibration of the NO_2 group, i.e. rocking, wagging and scissoring, contributes to the vibrational modes in the lower frequency region. The theoretically calculated values at 367, 731 and 842 cm^{-1} in the DFT values and 382, 763 and 857 cm^{-1} in the RHF values correspond to rocking, wagging and scissoring of the NO_2 vibrations. These findings are in good agreement with the results of our earlier report [15]. The scissoring mode of the CH_2 group gives rise to a characteristic band near 1465 cm^{-1} [14] in the IR and Raman spectra. In the present study, the band that appears at 1426 cm^{-1} in both IR and Raman spectra is assigned to the scissoring mode of the CH_2 group. The calculated values of 1430 and 1459 cm^{-1} in the DFT and RHF methods agree with the experimental values of CH_2 scissoring vibrations of nicorandil. The FTIR bands at 1170 and 1260 cm^{-1} and Raman bands at 1169 and 1248 cm^{-1} were ascribed to the CH_2 twisting mode of vibration. These observations are made in analogy with the literature values [14]. The other bending vibrations, i.e. HCH, CCH, ONO, CCC, CCO and CCN, are identified and assigned.

4.10 Thermodynamic properties

Several calculated thermodynamic parameters at room temperature are presented in Table 5. According to Koopmanns' theorem, ionisation potential (I) is the negative of the highest occupied molecular orbital (HOMO) energy, i.e. $I = -E_{HOMO}$, and affinity potential (A) is the negative of the lowest unoccupied molecular orbital (LUMO) energy, i.e. $A = -E_{LUMO}$, which are summarised in Table 5.

In general, the HOMO becomes less bound while the LUMO becomes more bound. From Table 5, it is concluded that the lowest energy gap was found at the DFT method. The variations in the entropy and zero-point vibrational energies seem to be insignificant. The thermal energy of nicorandil is found to be smaller in the DFT method.

Table 5. Theoretically calculated rotational constant, zero-point vibrational energy (ZPVE), entropy (cal/mol K), heat capacity (cal/mol K), thermal energy (kcal/mol), dipole moment, HOMO, LUMO and energy gap of nicorandil.

Thermodynamic parameters	B3LYP/6-31G(d,p)	RHF/6-31G(d,p)
Rotational constant (GHz)	2.17008	2.2875
	0.1929	0.19567
	0.18939	0.19171
ZPVE (kJ/mol)	473.045	512.659
Entropy		
Total	122.337	117.867
Translational	41.945	41.945
Rotational	32.672	32.593
Vibrational	47.72	43.329
Heat capacity	48.708	44.792
Thermal energy	121.627	130.522
Dipole moment (Debye)	6.1354	7.0586
HOMO (eV)	7.14	9.92
LUMO (eV)	1.78	2.26
Energy gap (eV)	5.36	6.66

5. Conclusion

We present results on the structural and vibrational properties of nicorandil using mid-IR and Raman spectra. The theoretically calculated values of both bond lengths and bond angles of the structures of the minimum energy were then compared with X-ray crystallographic data. The data obtained during the course of the present investigation show that a better agreement between the experimental and computed data is obtained using the DFT method B3LYP with the basis set 6-31G(d,p).

This study predicted that the vibrational frequencies of nicorandil could be successfully elucidated by the RHF and B3LYP methods using Gaussian program. The fitting between calculated and measured vibrational frequencies was achieved by these methods and the deviations between calculated and experimental values are quite small after scaling the frequencies. Therefore, this study confirms that the theoretical calculation of the vibrational frequencies for nicorandil is quite useful for determining the vibrational assignment and for predicting new vibrational frequencies.

The bond order and atomic charges of the title molecule have been studied by both RHF and DFT methods. The calculated normal-mode vibrational frequencies provide thermodynamic properties by way of statistical mechanics.

References

[1] J. Frampton, M.M. Buckley, and A. Fitton, *Review of nicorandil and pharmacology and therapeutic efficacy in angina*, Drugs 44 (1992), pp. 625–655.

[2] A. Markham, G.L. Prosker, and K.L. Goa, *Nicorandil. An updated review of its use in ischaemic heart disease with emphasis on its cardioprotective effects*, Drugs 60 (2000), pp. 955–974.

[3] N.C. Handy, C.W. Murray, and R.D. Amos, *Study of methane, acetylene, ethane, and benzene using Kohn–Sham theory*, J. Phys. Chem. 97 (1993), pp. 4392–4396.

[4] P.J. Stephens, F.J. Devlin, C.F. Chavalowski, and M.J. Frisch, Ab initio *calculation of vibrational absorption and circular dichroism spectra using density functional force fields*, J. Phys. Chem. 98 (1994), pp. 11623–11627.

[5] F.J. Devlin, J.W. Finley, P.J. Stephens, and M.J. Frisch, Ab initio *calculation of vibrational absorption and circular dichroism spectra using density functional force fields: A comparison of local,*

Downloaded At: 17:09 14 January 2011

nonlocal, and hybrid density functional, J. Phys. Chem. 99 (1995), pp. 16883–16902.

[6] S.Y. Lee and B.H. Boo, *Density functional theory study of vibrational spectra of anthracene neutral and radical cation*, Bull. Korean Chem. Soc. 17 (1996), pp. 754–759.

[7] S.Y. Lee and B.H. Boo, *Molecular structure and vibrational spectra of 9-fluorenone density functional theory study*, Bull. Korean Chem. Soc. 17 (1996), pp. 760–764.

[8] G. Rauhut and P. Pulay, *Transferable scaling factors for density functional derived vibrational force fields*, J. Phys. Chem. 99 (1995), pp. 3093–3100.

[9] A.D. Becke, *Density-functional thermochemistry. III. The role of exact exchange*, J. Chem. Phys. 98 (1993), pp. 5648–5652.

[10] M.J. Frisch, G.W. Trucks, H.B. Schlegel, G.E. Scuseria, M.A. Robb, J.R. Cheeseman, J.A. Montgomery, Jr., T. Vreven, K.N. Kudin, J.C. Burant, J.M. Millam, S.S. Iyengar, J. Tomasi, V. Barone, B. Mennucci, M. Cossi, G. Scalmani, N. Rega, G.A. Petersson, H. Nakatsuji, M. Hada, M. Ehara, K. Toyota, R. Fukuda, J. Hasegawa, M. Ishida, T. Nakajima, Y. Honda, O. Kitao, H. Nakai, M. Klene, X. Li, J.E. Knox, H.P. Hratchian, J.B. Cross, C. Adamo, J. Jaramillo, R. Gomperts, R.E. Stratmann, O. Yazyev, A.J. Austin, R. Cammi, C. Pomelli, J.W. Ochterski, P.Y. Ayala, K. Morokuma, G.A. Voth, P. Salvador, J.J. Dannenberg, V.G. Zakrzewski, S. Dapprich, A.D. Daniels, M.C. Strain, O. Farkas, D.K. Malick, A.D. Rabuck, K. Raghavachari, J.B. Foresman, J.V. Ortiz, Q. Cui, A.G. Baboul, S. Clifford, J. Cioslowski, B.B. Stefanov, G. Liu, A. Liashenko, P. Piskorz, I. Komaromi, R.L. Martin, D.J. Fox, T. Keith, M.A. Al-Laham, C.Y. Peng, A. Nanayakkara, M. Challacombe, P.M.W. Gill, B. Johnson, W. Chen, M.W. Wong, C. Gonzalez, and J.A. Pople, *Gaussian 03, Revision A.1*, Gaussian, Inc., Pittsburgh PA, 2003.

[11] C. Lee, W. Yang, and R.G. Parr, *Development of the Colle–Salvetti correlation-energy formula into a functional of the electron density*, Phys. Rev. B 37 (1988), pp. 785–789.

[12] Y. Nawata, N. Terao, T. Terazono, K. Igusa, Y. Yutani, and K. Ochi, *Structure of N-[2-(nitrooxy)ethyl]nicotinamide*, Acta Cryst. C 43 (1987), pp. 2460–2462.

[13] A.P. Scott and L. Radom, *Harmonic vibrational frequencies: An evaluation of Hartree–Fock, Møller–Plesset, quadratic configuration interaction, density functional theory, and semiempirical scale factors*, J. Phys. Chem. 100 (1996), pp. 16502–16513.

[14] T. Vijayakumar, I. Hubert Joe, C.P. Reghunadhan Nair, and V.S. Jayakumar, *Vibrational spectral studies on charge transfer and ionic hydrogen-bonding interactions of nonlinear optical material L-arginine nitrate hemihydrate vibrational spectral studies on charge transfer and ionic hydrogen-bonding interactions of nonlinear optical material L-arginine nitrate hemihydrate*, J. Raman Spectrosc. 40 (2009), pp. 18–30.

[15] S. Azhagiri, G.R. Ramkumaar, S. Jayakumar, S. Kumaresan, R. Arunbalaji, S. Gunasekaran, and S. Srinivasan, *Theoretical and experimental studies of vibrational spectra and thermal analysis of 2-nitroaniline and its cation*, J. Mol. Model. 16 (2010), pp. 87–94.

[16] C. Floare, S. Astilean, M. Bogdan, and O. Cozar, *DFT structure optimization and vibrational spectra of the photochromic 2-(2′,4′-dinitrobenzyl)pyridine*, Rom. J. Phys. 50 (2005), pp. 815–829.

[17] B. Venkatram Reddy and G. Ramana Rao, *Normal coordinates treatment of some pyridine*, Indian J. Phys. 76B (2002), pp. 473–477.

[18] N. Sundaraganesan, S. Ayyappan, H. Umamaheshwari, and B. Dominic Joshua, *FTIR, FT-Raman spectra and* ab initio*, DFT vibrational analysis of 2,4-dinitrophenylhydrazine*, Spectrochim. Acta A 66 (2007), pp. 17–27.

Downloaded At: 17:09 14 January 2011